*31st EPS Conference on Plasma Phys. London, 28 June - 2 July 2004 ECA Vol.**28G**, P-1.202 (2004)*

Island compensation coils in W7-X

C. Nührenberg[1], A.H. Boozer[2]

[1]*Max-Planck-Institut für Plasmaphysik, Teilinstitut Greifswald*
IPP-EURATOM Association, D-17491 Greifswald, Germany
[2] *Columbia University, New York, New York 10027, USA*

I. INTRODUCTION

The divertor of the Wendelstein 7-X (W7-X) stellarator will use *natural* island chains that appear at low-order rationals of the rotational transform near the plasma edge (5/5 in the standard, 5/4 in the high-ι, and 5/6 in the low-ι case). The W7-X magnet system includes five pairs of control-saddle coils, which may be used for a fine adjustment of these islands for optimum divertor operation. The additional inclusion of Island Compensation Coils (ICCs) in the W7-X magnet system would allow for the magnetic compensation of the most important perturbations (1/1, 2/2, and 3/3) that could arise from errors in coil manufacturing or positioning and might impede proper divertor operation. ICCs would also allow controlled studies of the effects of error-fields on W7-X plasmas: a study, for example, of the importance of plasma shielding of error-fields. In this study ICCs outside the cryostat are investigated. Their assets are: (i) that they utilize the distance possible because of the slow drop-off of the fields compensating the more dangerous low-m error-fields; (ii) that they may possibly be realized at a late stage in W7-X, even after the machine is operational; (iii) that they need not be accurately constructed since their distance from the plasma ensures all but the lowest Fourier components will be filtered out through the exponential decay of curl-free fields of short wavelength; and (iv) their feasibility for a fusion power plant.

CASE		I	#1	#2	#3	#4	#5	A	B	S
		[MA]	F							
SC	standard	1.60	1	1	1	1	1	0	0	0
HI	high-ι	1.60	1	1	1	1	1	-0.22	-0.22	0
LI	low-ι	1.32	1	1	1	1	1	+0.24	+0.24	0

Fig. 1. *Current loads for the three W7-X variants studied here. Columns #1 to #5 refer to the five modular-coil types, A and B to the two auxiliary-coil types, and S to the saddle-coil type.*

II. DETAILS OF STUDY

Three magnetic scenarios are studied here: (i) the standard case with rotational transform $5/6 < \iota < 5/5$, (ii) the high-ι case with $5/5 < \iota < 5/4$, and (iii) the low-ι case with $0.72 < \iota < 5/6$. The table of Fig. 1 lists the current loads needed to obtain these operation cases [1]. The magnetic topology of the three cases is shown in the left frames of Figs. 2, 3, and 4. (As will be seen below, the middle frames show perturbed and the right frames the restored cases with the ICCs activated). These particular triangular cross-sections are at $\varphi_{cyl} = 180^o$. Because of the specific selection of their starting points, the field lines do not fill the islands near the plasma boundary (5/5 in Fig. 2, 5/4 in Fig. 3). In the 5/6 case (Fig. 4), there are starting points for the field line tracing inside the island chain. In Figs. 2 and 3, a control surface is marked in red. Its purpose is explained below. The island chains' locations are approximately fixed in space, which is important for the divertor to work in all magnetic scenarios.

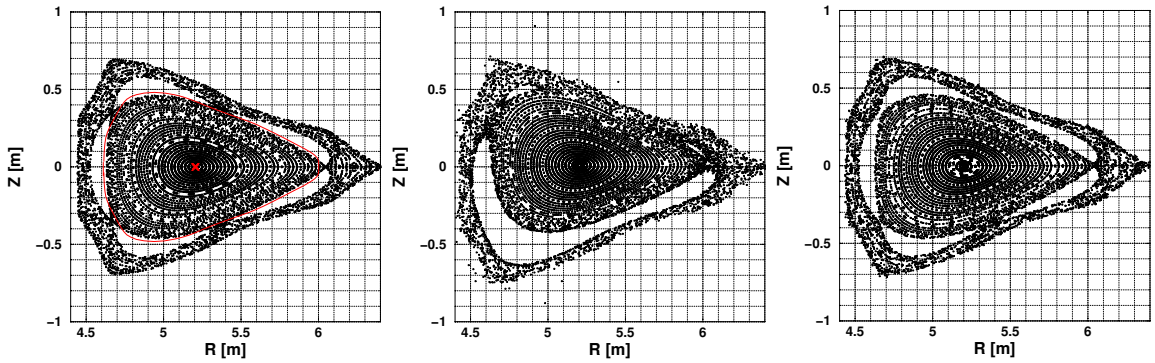

Fig. 2. *Left: Field-line tracing in the vacuum field of the W7-X standard case. A toroidal control surface for evaluating resonant field components and the location of the magnetic axis are marked in red. The cross section is at* $\varphi_{cyl} = 180^{o}$*. Middle: Same as left, but including a field perturbation due to a misalignment of the modular coils #3, #18, and # 44 (perturbation type CR). The relative strength of some resonant error-field harmonics is given in Fig. 5. Right: The perturbation CR is compensated by the trapezoidal ICCs at R=5.35 m and a=2.20 m and the current loading as given in line 1 of the table in Fig. 6.*

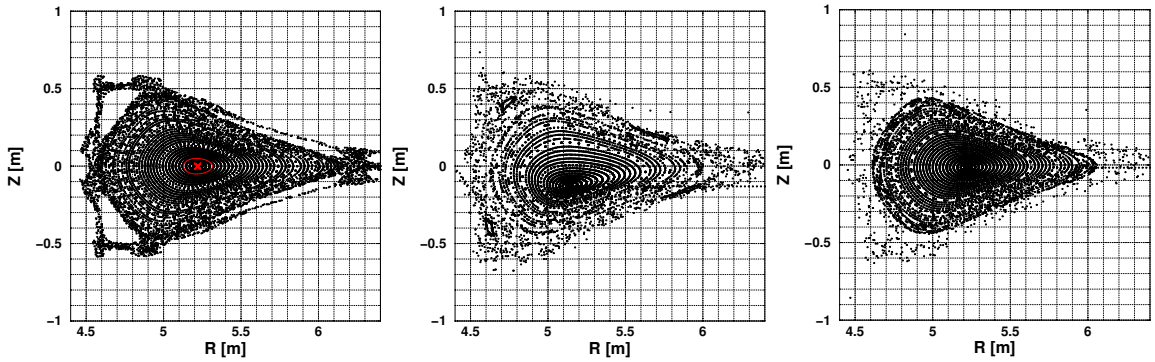

Fig. 3. *Left: Same as Fig. 2, but for the high-*ι *W7-X variant: 5/5 <* ι *< 5/4. The 5/4 islands are not filled by fields lines because of the specific choice of their starting points. Middle: Same as left, but including a field perturbation due to a misalignment of the modular coils #3, #18, and # 44 (perturbation type CR). Right: The perturbation CR is compensated by the helical ICCs at R=5.35 m and a=2.20 m and the current loading as given in line 2 of the table in Fig. 6.*

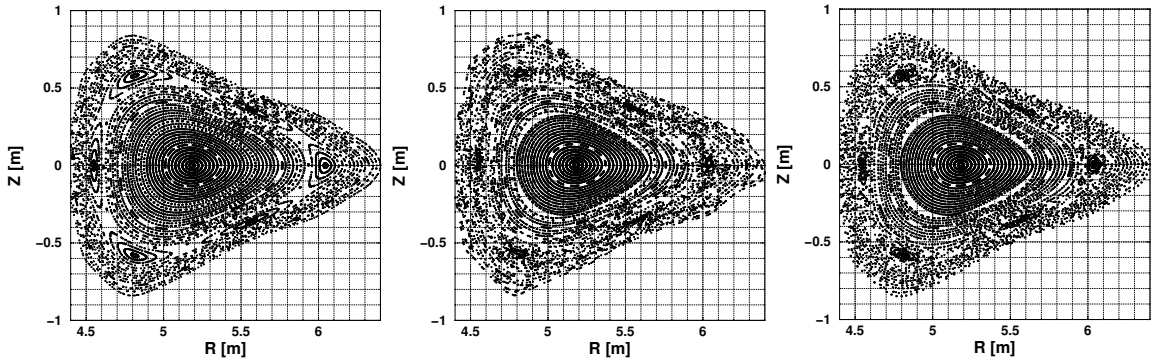

Fig. 4. *Left: Same as Fig. 2, but for the low-*ι *W7-X variant: 0.72 <* ι *< 5/6. A large area of magnetic surfaces exists outside the 5/6 islands. Middle: Same as left, but including a field perturbation due to a misalignment of the modular coils #3, #18, and # 44 (perturbation type CR). Right: The perturbation CR is compensated by the helical ICCs at R=5.35 m and a=2.20 m and the current loading as given in line 2 of the table in Fig. 6.*

The introduction of a perturbation field destroys the fivefold symmetry of the magnetic field. Three types of perturbations are studied here: the effect of (i) a modular coil misalignment (TYPE: CR); (ii) bad modular coil shapes (TYPE: CS); and (iii) the misalignment of complete modular coil modules (TYPE: MM). For the perturbation CR, the modular coils #3, #18, and #44 (of in total 50 modular coils) have been rotated around vertical axes through their geometric centers as to move their individual outermost peripheral points by 0.04 m, 0.03 m, and 0.03 m. The perturbations CS and MM are described in detail in Ref. 2. In the table of Fig. 5, the relative perturbation field harmonics, that are resonant at $\iota = 1$, are listed for m upto 5 (data for the standard case with B_0 = 2.78 T). Perturbation CR is dominantly m=1, n=1 with a marked (3,3) contribution. Perturbation CS is dominantly m=2, n=2 and shows a mixture of competing harmonics upto m=4. Perturbation MM is clearly m=1, n=1, with the higher-m components small.

CASE: SC		δB_{11}	δB_{22}	δB_{33}	δB_{44}	δB_{55}
TYPE		$[10^{-4}]$				
CR	coil rotation	1.84	0.52	0.89	0.28	0.30
CS	bad coil shape	0.92	1.67	0.79	1.00	0.24
MM	module misalignment	3.06	0.48	0.51	0.12	0.03

Fig. 5. *Relative error-field harmonics,* B_0 = 2.78 *T in the W7-X standard case at 1.6 MA.*

The middle frames of Figs. 2, 3, and 4 show the influence of the CR perturbation. In the standard case (compare Fig. 2), one large island and two smaller ones appear in the region of the unperturbed 5/5 island chain. The central part of the plasma appears to be unchanged, the location of the magnetic axis stays fixed. In the high-ι case (compare Fig. 3), the region of the 5/4 islands gets ergodized, the main change here is a dislocation of the magnetic axis. This is due to the near-unity rotational transform at the axis in the unperturbed case. The smallest influence of the error-field is seen in the low-ι case (middle frame of Fig. 4): The 5/6 islands stay in place, but get ergodized. Thin 3/4 and 4/5 island chains appear in the inner plasma region.

In this study, two ICC designs are compared: Lay-out T comprises ten trapezoidal loops, lay-out H ten helical windings. In both cases the ICCs have been arranged on a circular torus representing the outer cryostat wall. The dimensions are given by a major radius of R=5.35 m and a minor radius of a=2.2 m. Both lay-outs take into account $\iota = 1$ in the overall orientation of the ICCs.

III. RESULTS

With a Singular Value Decomposition method (SVD, [3]) and the use of a control surface the current loading for the ten ICCs has been determined. The table in Fig. 6 shows the current combinations which have been determined to approximately restore the perturbed fields. Standardly, the outer control surface of Fig. 2 has been used to evaluate the error-field harmonics and the harmonics of the ICC fields. Only in the high-ι case (HI) which has been perturbed by bad modular coil shape (CS) the inner control surface of Fig. 3 had to be used, because the compensation currents determined from the outer control surface showed the unfavorable effect of not completely restoring the magnetic axis location. In all the cases the error-field harmonics (m, m), $m = 1, \ldots 5$ have been used to determine the ICC currents. Three approximately restored magnetic fields are shown in the right frames of Figs. 2 to 4.

TYPE	ICC	ICC1	ICC2	ICC3	ICC4	ICC5	ICC6	ICC7	ICC8	ICC9	ICC10	$\sum \lvert \text{ICC} \rvert$
		[kA]										
CR	T	+ 2.7	- 1.4	-18.0	+ 5.5	+ 7.6	- 0.5	-19.9	+11.0	+ 1.1	+ 7.9	75.6
	H	- 2.2	- 5.9	- 2.0	+ 3.1	- 1.6	- 2.8	+ 4.4	+ 1.1	- 1.2	+ 4.2	28.5
CS	T	- 8.5	- 6.8	-12.7	+ 7.5	+ 2.3	- 9.5	- 9.0	-15.4	- 0.6	+ 6.4	78.7
	H	+ 3.7	+ 4.9	- 2.2	- 3.9	+ 1.6	+ 2.8	+ 1.2	+ 1.0	- 2.5	- 4.8	28.6
MM	T	- 9.1	+12.1	-12.0	- 6.9	- 1.9	- 0.6	-12.8	+ 1.3	- 1.7	+ 5.6	64.0
	H	+ 1.7	- 0.2	- 1.1	+ 3.8	+ 2.6	- 1.9	- 1.9	- 0.7	- 1.4	+ 0.7	16.0
HI-CS	T*	- 8.8	+13.5	- 1.7	-22.7	+10.1	- 4.6	- 2.5	+ 2.1	+ 0.1	- 1.5	67.6
	H*	- 0.7	- 4.3	+ 3.0	- 1.1	-10.2	+ 1.4	+10.0	- 8.0	-10.5	+ 6.5	55.7

Fig. 6. *Current loads for the two ICC lay-outs used here. TYPE indicates which perturbation is compensated: CR for rotation of coils #3, #18, and #44; CS for bad modular coil shape; MM for misalignment of complete module; the entry T in column ICC indicates the trapezoidal and the entry H the helical compensation coils. Standardly, the outer control surface (see Fig. 2) has been used. Exceptions are marked with* $*$ *and use the inner control surface of Fig. 3.*

In the low-ι case, the ICC-current loads of Fig. 6 have been scaled by the factor $1.32/1.6$ (compare Fig. 1) and show satisfactory results, although the control surface is not explicitly adapted to the low-ι magnetic topology.

IV. SUMMARY

The error-field resulting from the misalignment of complete modular-coil modules (type MM) with its clearly dominating m=1, n=1 harmonic is best amenable to compensation by ICCs located outside the cryostat. The error-field resulting from bad modular coil shape (type CS) with its marked m=4, n=4 contribution may only less satisfactorily be compensated by ICCs located outside the cryostat, since the exponentially decaying higher harmonics of the compensation field are less effective at larger distances. In this case the outside-cryostat ICCs might be combined with the inside-cryostat control-saddle coils. Typically, the helical ICCs need the lower individual currents, the highest value occurring is 5.9 kA, not accounting for the case HI-CS with the inner control surface. In this case the highest individual current is 10.5 kA. For the trapezoidal ICCs the highest individual current is below 25 kA.

[1] Wendelstein 7-X phase-2 proposal, chap. 2, p.3
[2] J. Kisslinger's documentation, private communication.
[3] G.H. Golub, Ch.F. van Loan, Matrix Computations, (The John Hopkins University Press, Baltimore, USA), 1983.